Theoretical phase diagram of ultrathin films of incipient ferroelectrics

A. R. Akbarzadeh[1,2], L. Bellaiche[2], Jorge Íñiguez[3], and David Vanderbilt[4]
[1]*Department of Materials Science and Engineering, University of California, Los Angeles, P.O. Box 951595, Los Angeles, California 90095-1595, USA*
[2]*Physics Department, University of Arkansas, Fayetteville, AR 72701, Arkansas, USA*
[3]*Institut de Ciencia de Materials de Barcelona (ICMAB-CSIC), Campus UAB, 08193 Bellaterra, Spain and*
[4]*Department of Physics and Astronomy, Rutgers University, Piscataway, New Jersey 08854-8019, USA*
(Dated: April 30, 2007)

We have used a first-principles-based scheme to compute the temperature-versus-misfit strain "Pertsev" phase diagram of ultrathin films of *incipient* ferroelectric $KTaO_3$. Our results suggest that, at variance with the bulk material, $KTaO_3$ ultrathin films cannot be described as quantum paraelectrics. Rather, the behavior of the films is largely determined by surface/interface effects that favor ferroelectricity and the imperfect screening of the depolarizing fields. This leads to Pertsev phase diagrams that are qualitatively similar to those of *normal* ferroelectrics such as $BaTiO_3$.

The need for miniaturized devices and the quest for knowledge in nanoscience have led to a flurry of activities in ferroelectric thin films (see Refs. 1–3 and references therein). As a result, the influence of surface/interface effects and boundary conditions on their properties is now well documented. For instance, studies revealed that the strain arising from the substrate can lead to ferroelectric phases absent in the bulk[4–6], and that residual depolarizing fields can generate anomalous effects – such as stripe domains with remarkably small periods[7–9].

An important issue that remains to be fully understood concerns the properties of ferroelectric films made of incipient ferroelectrics, i.e., materials such as $SrTiO_3$ and $KTaO_3$ for which the bulk phase ferroelectricity is suppressed by quantum fluctuations[10–12]. The pioneering work in Ref. 13 revealed the existence of room-temperature ferroelectricity in *strained* 500 Å-thick $SrTiO_3$ films, and can thus be taken to suggest that the coupling between strain and dipoles tends to prevail over quantum effects in nanostructures. One may thus wonder what the effect (if any) of quantum zero-point vibrations is in ultrathin films made of incipient ferroelectrics. In particular, the following questions are, to the best of our knowledge, currently unanswered: (1) Can quantum fluctuations suppress some phases in these films, and, if so, which ones? (2) For zero misfit strain, are the films paraelectric or ferroelectric? (3) What are the consequences and signatures of the zero-point motion of the ions in a film experiencing a depolarizing field?

The aim of this Letter is to answer these questions by predicting the temperature-versus-misfit strain phase diagrams of $KTaO_3$ ultrathin films under different electrical boundary conditions.

Here, we use a first-principles-based effective Hamiltonian approach to study $KTaO_3$ ultrathin films grown along the [001] pseudo-cubic direction (chosen to be along the z-axis), having K-O terminated surfaces/interfaces, and being 28 Å thick. The films are modeled by $10\times10\times7$ supercells that are periodic along the x- and y-axes (which lie along the [100] and [010] pseudo-cubic directions, respectively) and contain seven TaO_2 (001) layers stacked along the non-periodic z-axis. We make use of an effective-Hamiltonian expansion $\mathcal{E}_{\rm Heff}(\mathbf{u}_{\rm i}, \mathbf{v}_{\rm i}, \eta)$, where the $\mathbf{u}_{\rm i}$ are the local soft-mode amplitudes in the unit cell i of the film (such that $Z^*\mathbf{u}_{\rm i}$ yields the local electrical dipole), $\{\mathbf{v}_{\rm i}\}$ are the inhomogeneous strains within the supercell[14], and η is the homogeneous strain tensor. The latter is relevant to mechanical boundary conditions since epitaxial (001) films are associated with the freezing of some components of η, i.e., $\eta_6=0$ and $\eta_1=\eta_2=\delta$, with δ being the value forcing the film to adopt the in-plane lattice constant of the substrate[5,6,8]. In practice, $\delta=(a_{\rm sub}-a_{\rm KTa})/a_{\rm KTa}$, where $a_{\rm sub}$ is the in-plane lattice parameter of the substrate and $a_{\rm KTa}=3.983$ Å is the 0 K cubic lattice constant of bulk $KTaO_3$ used in Ref. 11.

The analytical expression[14] and first-principles-derived parameters[11] for this $\mathcal{E}_{\rm Heff}$, the intrinsic effective-Hamiltonian energy of the film, are those of *bulk* $KTaO_3$, except that here we use the formula for the dipole-dipole interactions for thin films under ideal open-circuit (OC) boundary conditions derived in Refs. 15 and 16. Such electrical boundary conditions naturally lead to the existence of a maximum depolarizing field inside the film (denoted by $\mathbf{E}_{\rm d}$) when the dipoles point along the [001] direction. To treat more general electrical boundary conditions in which there is partial screening of this depolarizing field, we actually minimize the total-energy function

$$\mathcal{E}_{\rm tot} = \mathcal{E}_{\rm Heff}(\mathbf{u}_{\rm i}, \mathbf{v}_{\rm i}, \eta) + \beta\mathbf{E}_{\rm d}\cdot\sum_{\rm i} Z^*\mathbf{u}_{\rm i}\ , \qquad (1)$$

where β is a screening parameter defined such that $\beta=0$ corresponds to ideal OC conditions, an increase in β lowers the magnitude of the resulting depolarizing field, and $\beta=1$ corresponds to ideal short-circuit (SC) conditions for which the depolarizing field vanishes. Note that $\mathbf{E}_{\rm d}$ is derived at an atomistic level[15], and is self-consistently updated during the simulations. Also note that, as in Ref. 4, our $\mathcal{E}_{\rm tot}$ assumes a simple truncation, at the surface/interface layers, of the interactions existing in bulk $KTaO_3$. Such approximation results in an enhancement of the surface/interface polar modes for electrical boundary conditions close to SC, because the truncation removes short-range interactions that oppose the onset

of local dipoles. Interestingly, such enhancement of the surface/interface polar modes has been reported in some low-dimensional systems[17] (see, e.g, the *ab initio* results for $PbTiO_3$ films sandwiched by Pt electrodes[18] and the experimental and first-principles works in ferroelectric $BaTiO_3$ nanowires[19]).

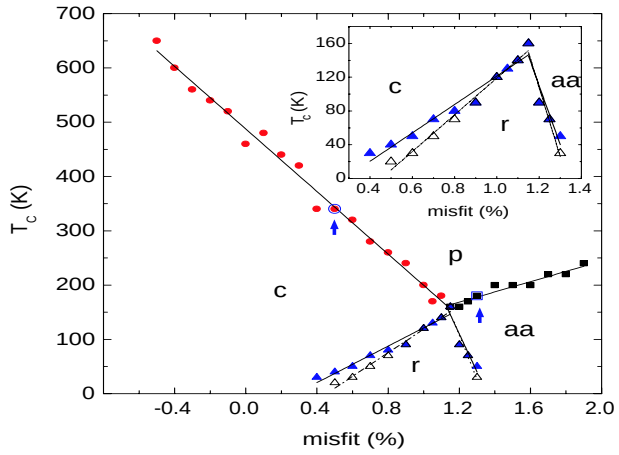

FIG. 1: Temperature *versus* misfit strain diagram of a 28 Å-thick $KTaO_3$ ultrathin film under ideal SC conditions ($\beta = 1$). Solid and open symbols refer to CMC and PI-QMC simulations, respectively. Serving as guides for the eyes, the solid and dashed lines are linear fits of the CMC and PI-QMC data, respectively. The inset shows a magnified view of the region in which the *r* phase occurs. PI-QMC simulations performed at temperatures higher than 100 K, at 0.5 % and 1.3 % misfit tensile strains, are indicated with arrows in Fig. 1, and reveal that the high-temperature *p*–to-*c* and *p*–to-*aa* phase transitions are unaffected by quantum fluctuations.

As in Ref. 11, $\mathcal{E}_{\rm tot}$ is used in two different kinds of Monte-Carlo (MC) simulations: classical Monte Carlo (CMC)[20], which does not take into account zero-point vibrations, and path-integral quantum Monte Carlo (PI-QMC)[21–23], which includes the quantum-mechanical zero-point motions. We typically used 30,000 MC sweeps to thermalize the system and 70,000 more to compute averages, except at low temperature in PI-QMC where more statistics are needed.

Figure 1 displays the "Pertsev" (that is, the temperature *versus* misfit strain δ) phase diagram for the 28 Å-thick $KTaO_3$ thin film under ideal SC conditions, as resulting from CMC and PI-QMC simulations. One can clearly see that both kinds of simulations generate the four phases that also appear in the Pertsev diagram of (001) $BaTiO_3$ ultrathin films[4,6]. These phases are: a paraelectric *p* state at high temperatures; a ferroelectric tetragonal *c* phase for intermediate temperatures and compressive and weakly tensile strains, having a polarization lying along the [001] growth direction; a ferroelectric orthorhombic *aa* phase for low temperatures and large tensile strains, in which the polarization is parallel to the in-plane [110] direction; and a ferroelectric monoclinic *r* phase for the lowest temperatures and intermediate tensile strains, for which the polarization direction continuously rotates from [001] to [110] as δ increases.

Figure 1 further displays four remarkable features. (1) Quantum effects begin to appear at temperatures below ≈ 100 K. As a result, the *c*–to–*r* and, to a lesser extent, the *aa*–to–*r* phase boundaries are the *only* boundaries affected by quantum fluctuations. Essentially, there is a small reduction of the strain range in which the *r* phase occurs: in the low-temperature limit, it passes from about $+0.4\,\% \leq \delta \leq +1.3\,\%$ at a classical level to about $+0.5\,\% \leq \delta \leq +1.3\,\%$ when quantum fluctuations are included. (2) As in $BaTiO_3$ ultrathin films[4,6], the *p*, *c*, *aa*, and *r* phases *meet* at a single four-phase point, which occurs here at a temperature of about 160 K and a *tensile* strain of about 1.12 % for both CMC and PI-QMC simulations[24]. (3) The phase diagram is asymmetric with respect to zero misfit strain. Such an asymmetry is hinted in experiments on $Ba_{0.5}Sr_{0.5}TiO_3$ films[25] and is related to the enhancement of the z-component of the local dipoles at the surfaces/interfaces[26]. (4) For zero misfit strain, the paraelectric–to–*c* transition occurs at about 460 K for both CMC and PI-QMC simulations. This high transition temperature ($T_{\rm C}$) starkly contrasts with the behavior of the bulk material, for which the paraelectric–to–ferroelectric transition occurs at about 30 K at a classical level and vanishes when quantum effects are considered[11]. The physical origin of such a high $T_{\rm C}$ lies on the above mentioned dipole enhancement at the surface/interface of the films. The striking consequence of such an enhancement is that these ultrathin films are no longer incipient ferroelectrics, but display a Pertsev phase diagram that is in essence identical to that of a normal ferroelectric like $BaTiO_3$.

We now discuss how depolarizing fields, always present in reality as, e.g., the metallic electrodes are never ideal[27], affect the Pertsev phase diagram of $KTaO_3$ ultrathin films. Here, we have chosen $\beta = 0.96$ in Eq. (1), consistent with the *ab initio* studies of Sai *et al.*[18], which found this kind of cancellation of the depolarizing field in some films. The resulting Pertsev diagram is shown in Fig. 2, for both CMC and PI-QMC simulations. By comparing the CMC results from Figs. 1 and 2, it is clear that the depolarizing field tends to suppress the z-component of the polarization, as expected. Indeed, this effect dramatically decreases the *p*–to–*c* transition temperatures; for instance, the transition occurs around 60 K at zero misfit strain, i.e., the $T_{\rm C}$ is 400 K lower than the one obtained for ideal SC. It also considerably extends the region of small tensile strain associated with the *aa* phase and significantly narrows the *r-phase* region. As a result, the phase diagram becomes more symmetric around the zero misfit strain and the four-phase point of Fig. 1 shifts towards lower temperature (about 50 K for CMC simulations[24]). As shown in Fig. 2, such a small transition temperature implies that the quantum fluctuations (which are appreciable only at temperatures below 120 K, and become more pronounced as the temperature decreases) have two effects that do *not* occur in the film under SC

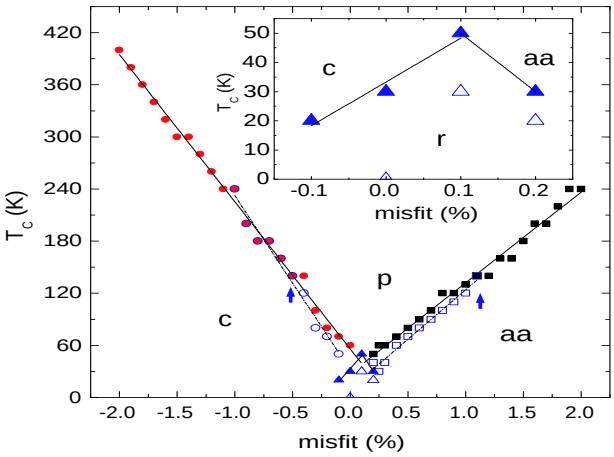

FIG. 2: Temperature *versus* misfit strain diagram of a 28 Å-thick ultrathin film $KTaO_3$ under a residual depolarizing field (β=0.96). Solid and open symbols refer to CMC and PI-QMC simulations, respectively. The solid and dashed lines are linear fits of the CMC and PI-QMC data, respectively, and are guides for the eyes. The inset is a magnification of the region in which the *r* phase occurs, with the PI-QMC data point for the *c*–to–*r* transition temperature at zero misfit strain being a guess resulting from the interpolation of the PI-QMC simulations for the lowest computed temperatures.

conditions. First of all, the zero-point vibrations now affect the *p*–to–*c* and *p*–to–*aa* phase boundaries (for small strain) – in addition to the boundaries involving the *r* phase. Secondly, quantum fluctuations significantly reduce the stability range of the *r*-*phase*. This suggests that, for slightly worse electrodes (i.e., for $\beta < 0.96$), quantum effects could well lead to the disappearance of the four-phase point in favor of a *three*-phase point in which "only" the *p*, *c*, and *aa* meet.

In summary, we have used a first-principles-based scheme and found that quantum fluctuations have a negligible effect for *ideal* electrodes: the phase diagram closely resembles what is found in films made of *strong* ferroelectrics, e.g. $BaTiO_3$. We have also simulated realistic (imperfect) electrodes and found that the corresponding depolarizing fields have a great impact on the calculated phase diagram; in particular, the transition temperatures of the *c* and *r* phases are significantly reduced. As a result, quantum mechanical effects become more important in this case, and may alter the phase diagram qualitatively, e.g., by suppressing the *r* phase.

We acknowledge useful discussions with George A. Samara and Kevin Leung. This work is supported by ONR grants N00014-01-1-0365, N00014-04-1-0413, and N00014-05-1-0054, by NSF grant DMR-0404335, and by DOE grant DE-FG02-05ER46188. J.I. thanks support from the Spanish Ministry of Science and Education (FIS2006-12117-C04-01) and FAME-NoE.

[1] M. Dawber, K. M. Rabe, and J. F. Scott , Rev. Mod. Phys. **77** 1083, (2006).
[2] J. F. Scott, Science **246**, 1400 (1989).
[3] I. Kornev, H. Fu and L. Bellaiche, J. Mater. Sci. **41**, 137 (2006).
[4] B.-K. Lai, I. Kornev, L. Bellaiche, and G. J. Salamo, Appl. Phys. Lett. **86**, 132904 (2005).
[5] N. A. Pertsev, V. G. Kukhar, H. Kohlstedt and R. Waser, Phys. Rev. B **67**, 054107 (2003).
[6] O. Diéguez *et al.*, Phys. Rev. B **69**, 212101 (2004).
[7] S. K. Streiffer et al., Phys. Rev. Lett. **89**, 067601 (2002).
[8] I. Kornev, H. Fu and L. Bellaiche, Phys. Rev. Lett. **93**, 196104 (2004).
[9] I. Ponomareva and L. Bellaiche, Phys. Rev. B **74**, 064102 (2006).
[10] R. Viana, P. Lunkenheimer, J. Hemberser, R. Bohmer and A. Loidl, Phys. Rev. B **50**, 601(R) (1994).
[11] A. R. Akbarzadeh, L. Bellaiche, K. Leung, J. Íñiguez, and D. Vanderbilt Phys. Rev. B **70**, 054103 (2004).
[12] B. Salce, J. L. Gravil, and L. A. Boatner, J. Phys.: Condens. Matter **6**, 4077 (1994).
[13] J. H. Haeni *et al.*, Nature **430**, 758 (2004).
[14] W. Zhong, D. Vanderbilt and K.M. Rabe, Phys. Rev. Lett. **73**, 1861 (1994); Phys. Rev. B **52**, 6301 (1995).
[15] I. Ponomareva, I. Naumov, I. Kornev, H. Fu, and L. Bellaiche , Phys. Rev. B **72**, 140102 (R) (2005).
[16] I. I. Naumov and H. Fu, cond-mat/0505497 (2005).
[17] At a quantitative level, our simple truncation may well be underestimating this enhancement for some choices of electrodes and overestimating it for others. At any rate, as the interesting effects resulting from our simulations are very pronounced, we are confident they can be taken as reliable qualitative predictions.
[18] N. Sai, A. M. Kolpak, and A. M. Rappe, Phys. Rev. B **72**, 020101(R) (2005).
[19] J. E. Spanier et al., Nano Lett. **6**, 735 (2006). .
[20] N. Metropolis, A. W. Rosenbluth, M. N. Rosenbluth, A.H. Teller, and E. T. Teller, J. Chem. Phys. **21**, 1087 (1953).
[21] W. Zhong and D. Vanderbilt, Phys. Rev. B **53**, 5047 (1996).
[22] J. Íñiguez and D. Vanderbilt, Phys. Rev. Lett. **89**, 115503 (2002).
[23] D. M. Ceperley, Rev. Mod. Phys. **67**, 279 (1995).
[24] The lines displayed in Figs. 1 and 2 do not intersect at an accurately defined strain-temperature four-phase point. This is partly because the transition lines are *linear* fits of our simulated data points, and also because we have a 10 to 20 K uncertainty in the predicted transition temperatures.
[25] S. Rios *et al.* J. Appl. Phys. **99**, 024107 (2006).
[26] For zero misfit strain, $\beta = 1$, and $T = 50$ K, both CMC and PI-QMC rendered $u_z \approx 0.041$ and 0.037 a.u. for surface/interface and inner layers, respectively. For $\beta = 0.96$, these values get reduced to 0.015 and 0.013 a.u., respectively, for CMC, and to 0.013 and 0.012 a.u., respectively, for PI-QMC. The corresponding magnitude of the local mode is 0.024 a.u. at $T = 20$ K in bulk $KTaO_3$, according to CMC.
[27] J. Junquera and P. Ghosez, Nature **422**, 506 (2003).